GEOLOGICA CARPATHICA, APRIL 2023, 74, 2, 181–194 https://doi.org/10.31577/GeolCarp.2023.07

Đurđevac Sands and the intraformational paleosoils (Podravina, N Croatia) are newly dated to Late Pleistocene/Holocene

LIDIJA GALOVIĆ[1], KOEN BEERTEN[2], NINA HEĆEJ[1,✉] and †HRVOJE POSILOVIĆ[1]

[1]Croatian Geological Survey, Sachsova 2, 10 000 Zagreb, Croatia; ✉nhecej@hgi-cgs.hr
[2]Belgian Nuclear Research Centre SCK CEN, 2400 Mol, Belgium

(Manuscript received July 26, 2022; accepted in revised form March 10, 2023; Associate Editor: Pavel Bosák)

Abstract: The Đurđevac Sands refer to an extensive sandy region south of the Drava River in northern Croatia, where it builds distinctive aeolian dunes. To date, their chronostratigraphical position has been based on stratigraphical inferences (superposition) without numerical and absolute age control. The recent discovery of a buried double paleosoil below and above aeolian dune sands in an abandoned sandpit (Draganci) have allowed the determination of the first absolute dates of the Đurđevac Sands. Field observations and laboratory analyses indicate that the degree of pedogenetic development of these paleosoils is very low. They appear to belong to the arenosol soil type, which is also the dominant recent soil type in the area. ^{14}C analysis of charcoal from the paleosoils indicated their development during the Bølling–Allerød interstadial, approximately between 14.7 ka and 12.9 ka, as opposed to previous claims that they would be exclusively Holocene in age. Therefore, this shows the need for a detailed investigation of the Đurđevac Sands. The sands and paleosoils likely witnessed a series of alternating phases of landscape stability and instability during the Late Glacial and Holocene. Such episodes are known to have occurred in other sandy regions of the Carpathian basin as well.

Keywords: Đurđevac Sands, paleosoil, aeolian dunes, Holocene, Pleistocene, Croatia

Introduction

The Đurđevac Sands (Croatian: Đurđevački Pijesci) refer to an area of partially-stabilized aeolian dunes in the eastern part of the town of Đurđevac, Northern Croatia (Fig. 1). The area is also called the Croatian Sahara or Bloody Sands, after its unique appearance in this part of the globe. Recently, the dunes of the Đurđevac Sands came to the focus of multidisciplinary investigations (Bašić & Feletar 2017). The local community shows a strong interest in exploring the Đurđevac Sands as promotion of a special geographic and botanical reserve.

In the absence of fossils, the Holocene age of the Đurđevac Sands was determined by the superposition principle (Hećimović 1987) as shown on the geological map of the area (Fig. 2). The aeolian sands, which discordantly overlay alluvial, marsh, and lake sediments, were thought to be the result of Holocene sedimentation processes. The geological map of the area predicted a Pleistocene age for loess and loess-like deposits only, which are predominantly found near the edge of the alluvial plain and the bordering slopes of the surrounding uplands (Fig. 2). These loess deposits have been the subject of detailed mineralogical, paleontological, chronological, geomorphological, paleopedological, and paleoclimatological studies (Bognar 2008; Galović et al. 2009, 2011, in press a; Galović 2014, 2016; Galović & Peh 2014; Rubinić et al. 2015, 2018; Wacha et al. 2018; Pola et al. 2020). However, in comparison with other inland dune sand areas, e.g., in western Europe (e.g., Vandenberghe et al. 2013), the chronostratigraphic position of the Đurđevac Sands is based on rather weak evidence. Therefore, the objective of this study is to describe the basic characteristics of the Đurđevac Sands, including intraformational soils, and establish the first geochronological framework for their formation. These results will serve as milestones for the correlation of sedimentological archives of climate and environmental changes that occurred in the continental part of Croatia (continental climate) with those in the Dinaric (Adriatic) part of Croatia, which is characterised by a Mediterranean climate (Romić et al. 2014; Banak et al. 2021; Galović et al. 2021, in press b; Hećej & Durn 2021).

Geological setting

In northern Croatia (Fig. 1), the sedimentary record is more or less continuous from the Neogene to the Quaternary and related to the sedimentary evolution of the Pannonian basin (Pavelić 2001), which was influenced by active tectonics during the Quaternary (Prelogović et al. 1998).

The Đurđevac Sands are found in the south-western marginal part of the Pannonian Basin System, next to the peri-alpine area. Alpine rivers, such as the Sava, Drava, and Mura, quickly change from erosional to aggradational mode soon after leaving peri-alpine Slovenia and form broad floodplains in Croatia. These floodplains are predominantly composed of Alpine material (Pirkhoffer et al. 2021; Zakwan et al. 2022).

CC BY-NC-ND

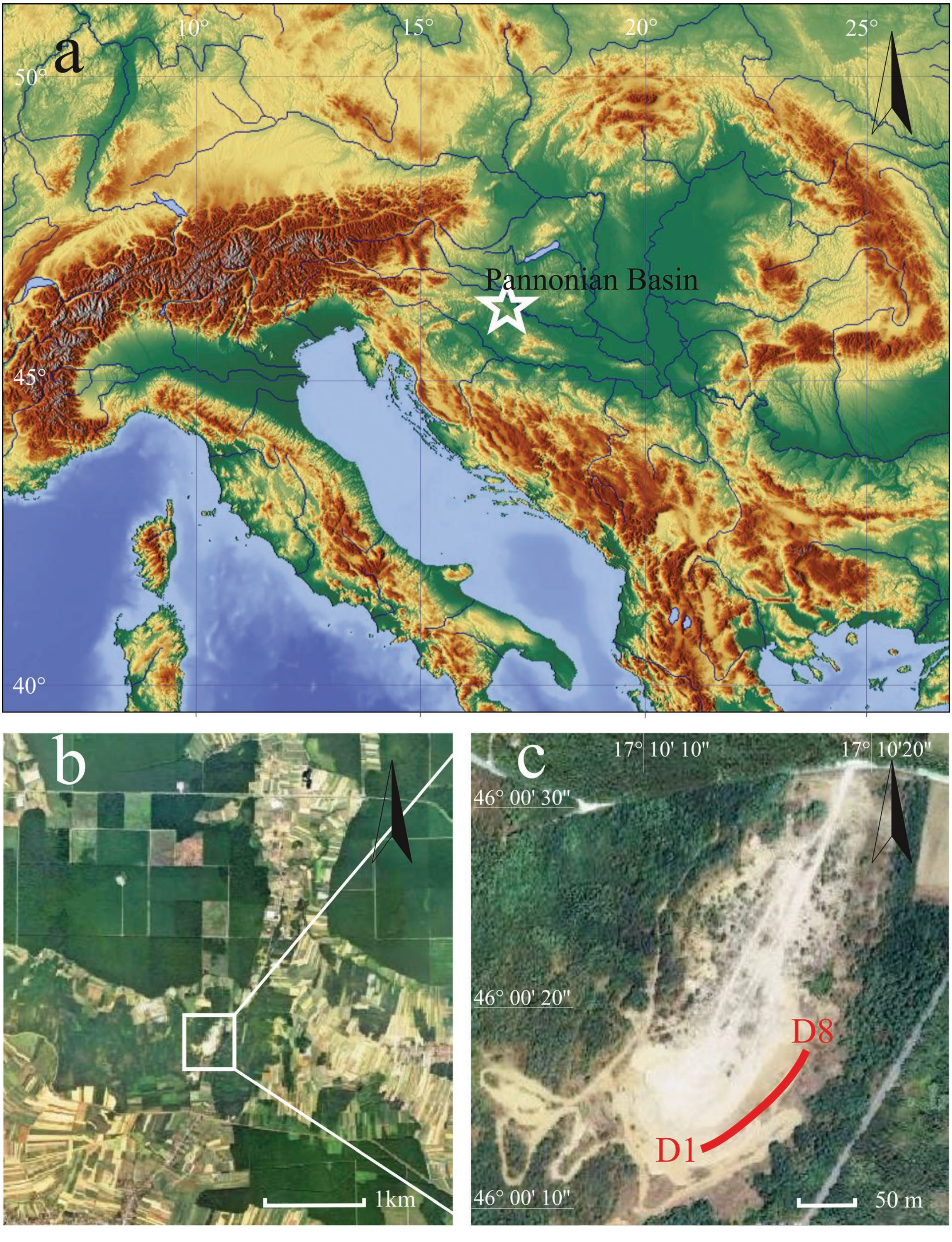

Fig. 1. a — Location of the Draganci area in Europe (Europe Relief Map, maps-for-free.com last accessed on June 21, 2022). **b** — Location of the sandpit in the wider Draganci area. **c** — Location of the investigated profile within the sandpit.

The Pleistocene sediment succession is closely related to the major rivers of the area (the Sava, Mura, and Drava Rivers) and their tributaries, and mainly consists of alluvial and aeolian sediments (Fig. 2; Wacha et al. 2013). Because of the domination of north-western winds in the area, the Đurđevac Sands were formed to the south of the Drava River.

During the Pleistocene glaciations, an increase in the volume of ice resulted in intense physical weathering of rocks in the Alps. This material was subsequently transported and additionally fragmented by newly formed rivers (such as the Drava River) to lowlands and floodplains (such as the Podravina area; Hećimović 1987). Sands and even finer material were deposited in these floodplains, however, strong north-western winds blew away the silty and clayey material. These natural separation processes resulted in the accumulation of medium-sorted sand with a high percentage of heavy mineral fraction (HMF; 7–54 %). The light mineral fraction (LMF) is dominated by quartz, and the HMF is dominated by garnet (Hećimović 1987; Galović & Posilović 2017). Within the dune sands, several darker horizons have been observed and interpreted as paleosoils, such that the sand must have been deposited in several separate phases of strong aeolian activity (Franjo 1997). The wider Đurđevac area is covered exclusively by Quaternary sediments (Hećimović 1987).

According to Hećimović (1987), these sands were repeatedly resedimented by winds and formed dunes during the Holocene: the so-called Đurđevac Sands (Fig. 2). The Đurđevac Sands (symbol ‘p’ in Fig. 2) are discordantly situated on the Pleistocene loess of the Bilogora Mt. slopes (‘l’), as well as in the Drava River Valley on the assumed Holocene sands and gravels of the second alluvial terrace (‘a_2’) and partially on marshy sediments (‘b’). The age of the Đurđevac Sands was thus determined by the superposition principle, based on the assumed Holocene age of the underlying material in the Drava River Valley (‘a_2’ and ‘b’) and the assumed Pleistocene age of the underlying material near the Bilogora Mt. slopes (‘l’).

Methods

Field methods

Field observations and sampling were performed in the disused sandpit Draganci (46°00’09”N, 17°10’14”E; Figs. 1, 2). The investigated paleosoils were unveiled along a 15 m long horizontal profile at eight different positions (D1 to D8; Fig. 3) to investigate their lateral extension. In addition, two vertical sequences were unveiled to investigate the pedo-sedimentological record. Based on field observations (grain size, colour, structure, texture), two horizons (D5a and D5b) in trench D5 were distinguished, investigated, and sampled, as well as nine horizons in trench D6 (D6a–D6i; Fig. 3). To reduce the influence of recent weathering and vegetation, at least 0.5 m of the outcrop surface was removed. Colour, grain size, structure, texture, bioturbations, and the presence of charcoal were described based on field observations.

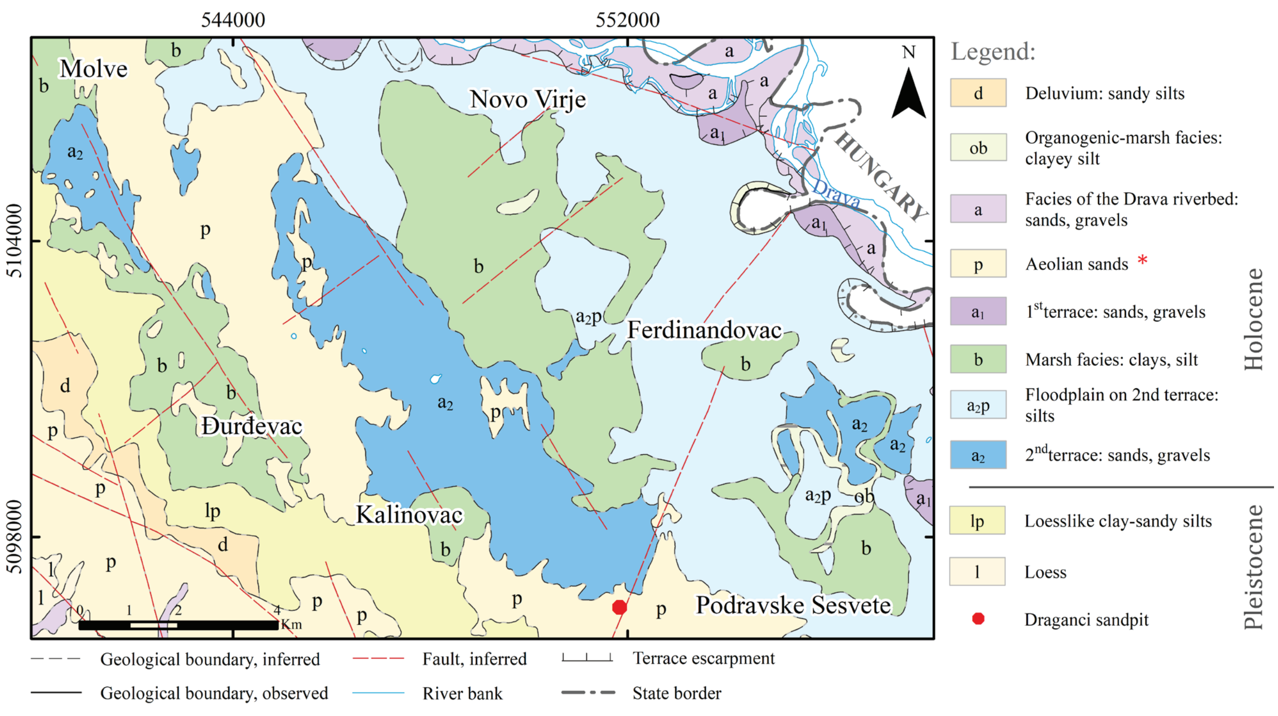

Fig. 2. Geological map of the area (after Hećimović 1988). The Đurđevac Sands correspond with the assumed Holocene aeolian sands indicated by ‘p’. The red asterisk is added to indicate that these sands are proven to be at least partially Late Pleistocene in age, as shown in this paper. The coordinate system of this map is EPSG:3765 – HTRS96.

Laboratory methods

Grain size and morphologic analysis of grains

Initially, samples were air-dried at a temperature below 40 °C for approximately one month. Particle-size analyses were performed at the Croatian Geological Survey (HGI-CGS) by sieving (1.25; 0.9; 0.45; 0.25; 0.125 and 0.09 mm size-fractions) and using the pipette method, and preceded by the removal of soil organic matter with H_2O_2, carbonates with 4 % HCl and dispersion with Na_2SiO_3 (HRN ISO 11277:2011) as described in Galović et al. (2009, 2011). Subsequently, the median (Md), sorting coefficient (So) and skewness (Sk) were calculated from these fractions (Galović 2014) with:

$$So = \sqrt{\frac{Q_3}{Q_1}} \tag{1}$$

and

$$Sk = \frac{Q_1 * Q_3}{(Md)^2} \tag{2}$$

with Q_1 being the 25th percentile and Q_3 the 75th percentile.

Finally, shapes of grains (sphericity and roundness) were analysed on fractions 1–0.5, 0.5–0.25, 0.25–0.125 and 0.125–0.09 mm to reconstruct their transport history. Sphericity and roundness were estimated using the graphical table from Krumbein & Sloss (1963).

Organic matter and calcium carbonate content

The proportion of organic matter (%) was determined gravimetrically. Porcelain pots were annealed at a temperature of 450 °C and filled with sample material with a weight of a minimum of 0.5 g and left overnight in an oven at 110 °C. The samples were then submerged in a 30 % hydrogen peroxide solution, in an amount sufficient to cover the entire sample. The sample was then annealed for 6 hours at 450 °C. The cooled samples were weighed and the organic matter was accordingly calculated.

The content of calcium carbonate (% $CaCO_3$) in the sample was determined volumetrically using the SCM1 Calcimeter. The weighed samples were added to an Erlenmeyer flask with the use of distilled water. The hydrochloric acid (4 mol/L HCl p.a.) was put into a test tube and placed inside the Erlenmeyer flask containing the suspended sample. After the flask was sealed, the reaction of hydrochloric acid and the sample was initiated, resulting in the release of carbon dioxide (CO_2), which was collected and measured by the difference in the volume of water registered in the burette. Based on the reading of the displaced volume of water, the calcium carbonate content (% $CaCO_3$) of the sample was calculated.

Radiocarbon dating (^{14}C)

Charcoal fragments that were extracted from the intercalated paleosoils were picked from the central part of the soils for two individual samples and submitted for radiocarbon dating. They were pre-treated according to a standard acid-base-acid protocol, combusted to oxidize organic matter to CO_2, reduced back to graphite, pressed into the cathode, and measured by accelerator mass spectrometry (AMS) in Direct AMS (Division of Accium Biosciences, Seattle, Washington, USA). A beam of C ions is produced by bombarding the surface of a graphite sample with Cs^+ ions. As such, the C beam is accelerated, focused, and split into 14, 13, and 12 amu beams. Results of the AMS analyses were also corrected for isotopic fractionation with an unreported $\delta^{13}C$ value (Taylor 1987) and presented in units of per cent modern carbon (pMC). Radiocarbon ages (0 BP=AD 1950) were calibrated with OxCal4.4 online software using Bayesian analysis (Bronk Ramsey 2009) and based on the IntCal20 calibration curve for the northern hemisphere (Reimer et al. 2020).

Results

Field observations

Two very dark greyish-brown sandy-textured paleosoils are present in the dune sequence and bounded by the upper and lower dark brown line as can be seen in Fig. 3. These paleosoils lack any significant soil profile development. There are no clear diagnostic horizons, and they are bereft of subsurface clay accumulation (as observed from palpation). Oblique parallel laminated sand can be observed above and below the paleosoils. 3D reconstructions of the laminae show that they dip with an angle of 26.5°, and they seem to be organised in sets of more than 1 m thickness (Fig. 4c). Another view of the stratified sands overlying the paleosoil is shown in Fig. 4b and e. The pedocomplex is sandy-textured without lamination and intensively bioturbated. Further up the stratigraphic column, a slight change towards a more yellowish colour can be observed, as is exemplified at observation point D6d (Fig. 4f). Here as well, the lamination seems to be less pronounced.

The lower paleosoil (Đ2; Fig. 4a) is about 15 cm thick (119.05–119.20 meters above mean sea level (m a.s.l.)), and the upper paleosoil (Đ3; Fig. 4a) is about 40 cm thick (119.60–120.00 m a.s.l.). The upper border of the younger paleosoil is erosional and is not bioturbated. Thus, the original thickness of the younger paleosoil could not be verified. Other contacts of the paleosoils with underlying and overlying sands are intensively bioturbated, especially the lower paleosoil (Fig. 4a). Preserved bioturbations confirm that the paleosoils are *in situ*. At some lateral locations, the two paleosoils cannot be distinguished from each other, since they appear as a merged pedocomplex (Galović 2016) as detailed below.

Along the horizontal profile, according to the Munsell Soil Color Book (2013), the pedocomplex is brown (D1, D6g, and D8), dark brown (D2, D3, D5a, D6h, D7, and D8), and sometimes very dark brown (D4) with a small yellowish (D2 and D7) or greyish (D4) component (Table 1). Overall, the colour

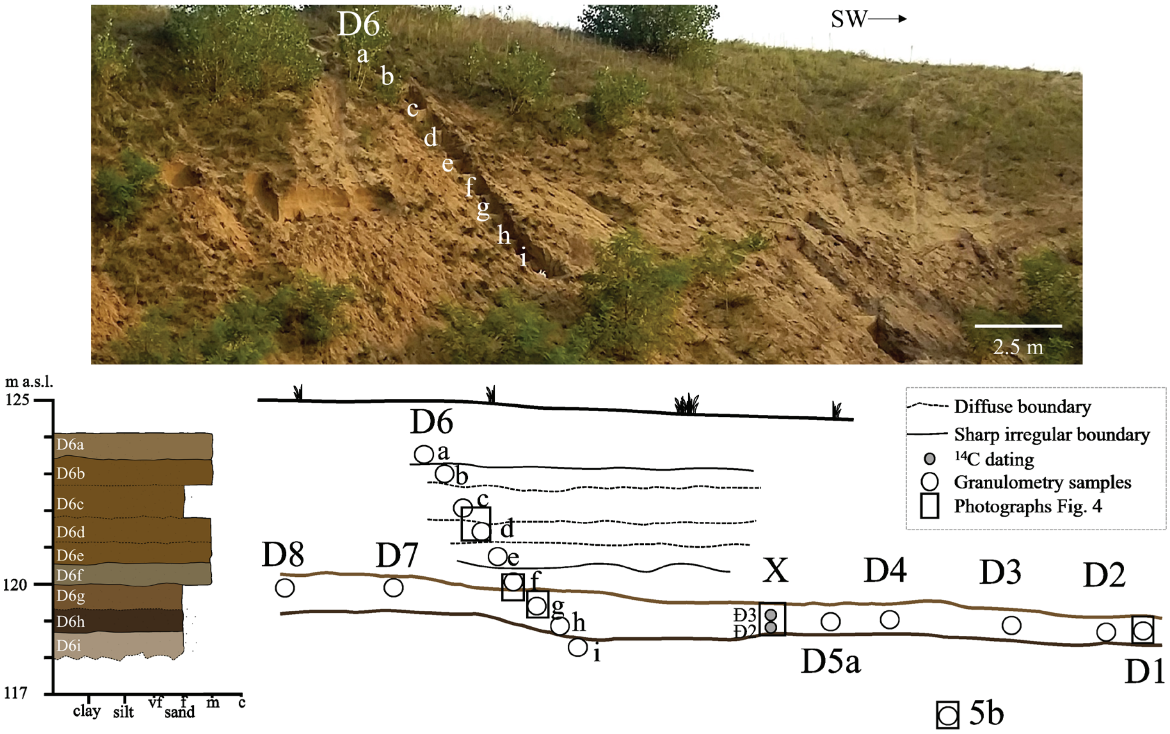

Fig. 3. Positions of outcrops and trenches sampled for detailed sedimentological analyses. Sedimentological log of the vertical profile D6. Pedocomplex samples are taken from positions D1, 2, 3, 4, 5a, 6g, 6h, 7, and 8.

of the paleosoils has a slightly less yellowish hue than the overlying and underlying sands and slightly less chroma (one unit less), and is also slightly darker (around one value unit or less). A dark colour might be caused by secondary precipitates, such as ferrous and/or manganese oxides or hydroxides. Another striking feature of the paleosoils is the complete absence of lamination. This can be seen in Fig. 4b, showing the contact between oblique parallel laminated dune sand overlying the bioturbated and unstratified paleosoil horizons (observation point D1).

Laboratory methods

Grain size and morphologic analysis of grains

According to the grain size measurements, the sand fraction dominates in all analysed samples, mostly between 95 and 100 % (Appendix 1, Fig. 5). This is also consistent with the median of the grain size distributions, which range from 0.18 mm to 0.26 mm. Medium and fine sand grains seem to represent the sand fraction equally. Therefore, most of the samples are classified as fine sand, or less frequently as medium sand (Wentworth 1922). Coarse sand particles are very rare (0–3 %). The clay and silt content is also very small — up to 7 % at most. The pedocomplex samples contain more fine and very fine sand than the strata above and below, up to ca. 70 % versus ca. 55 % respectively (Appendix 1), and also slightly more clay and silt (Appendix 1). This is also reflected in the slightly lower median for the paleosoil horizons compared to the sand layers, i.e., 0.21 mm and 0.24 mm respectively. In general, however, the differences are rather small, especially when the standard deviations on these results are taken into account (Appendix 1). As can be seen from Fig. 5a, there seems to be a slight coarsening trend in the southern direction along the horizontal profile (towards the position of sampling location 1).

The sorting coefficients (So) are moderate to very good, and they seem to be slightly higher in paleosoil horizons, 1.35 versus 1.28 (Appendix 1, Figs. 5b, 6b). The opposite trend can be seen for the skewnesses (Sk), 0.90 in soil horizons versus 0.94 in sand layers (Appendix 1, Figs. 5b, 6b). However, the differences are rather small and may appear insignificant given the standard deviation associated with these averages. On the contrary, the So/Sk ratio is higher in paleosoil horizons versus sand layers, i.e., 1.51 versus 1.36. In the vertical trench, this ratio clearly peaks in the paleosoil horizons (D6g and D6h).

A clear trend in organic matter content is lacking. There is no statistical difference between the percentages of organic matter in soil horizons versus sand layers (Appendix 2, Figs. 5c, 6c), although it has to be noted that the highest of all values (i.e., 1.13) is observed in one of the paleosoil samples (D6h). The inorganic carbon content, which was probed through analysis of the percentage of $CaCO_3$, seems to be systematically lower in paleosoil samples versus sand layers (Appendix 2, Figs. 5c, 6c). However, large variations exist within both groups, ranging between 0.17 % and 2.84 % in the former, and between 0.22 % and 7.89 % in the latter. An extraordinary trend seems to be present in the vertical profile (Fig. 6c), with the upper three samples showing values around 1 %, the four samples below showing very low (near zero) values, while towards the bottom of the profile, the inorganic carbon content rises drastically up to almost 8 %.

There is no significant difference in the shapes of grains between the analysed samples (Appendix 3). Both roundness (ranging between 0.16 and 0.27) and sphericity (ranging between 0.53 and 0.85) show a declining trend with smaller grain sizes within most of the individual samples.

Grain size fractions 0.25–0.09 mm are almost exclusively composed of angular grains. Exceptions are samples D1, D5b, and D6a (Appendix 3) with subangular grains in the very fine fraction (0.125–0.9 mm). Angular and subangular grains equally represent medium-sized sand grains, although the rare coarse sand grains (Appendix 3) tend to be subangular. Taking into account the grain size composition of the samples (dominant medium- and fine-grained sand; Appendix 3), the Đurđevac Sands are composed of angular and rarely subangular sand grains.

Grains from paleosoil samples D1 to D4 have moderate sphericity, while sample D5a has high sphericity. Samples D5b and D6a–e have moderate sphericity. Low sphericity is detected in samples D6f–i, D7 and D8. It thus seems that samples in the northern part, as well as the lower part of the profile, are characterised by low sphericity grains.

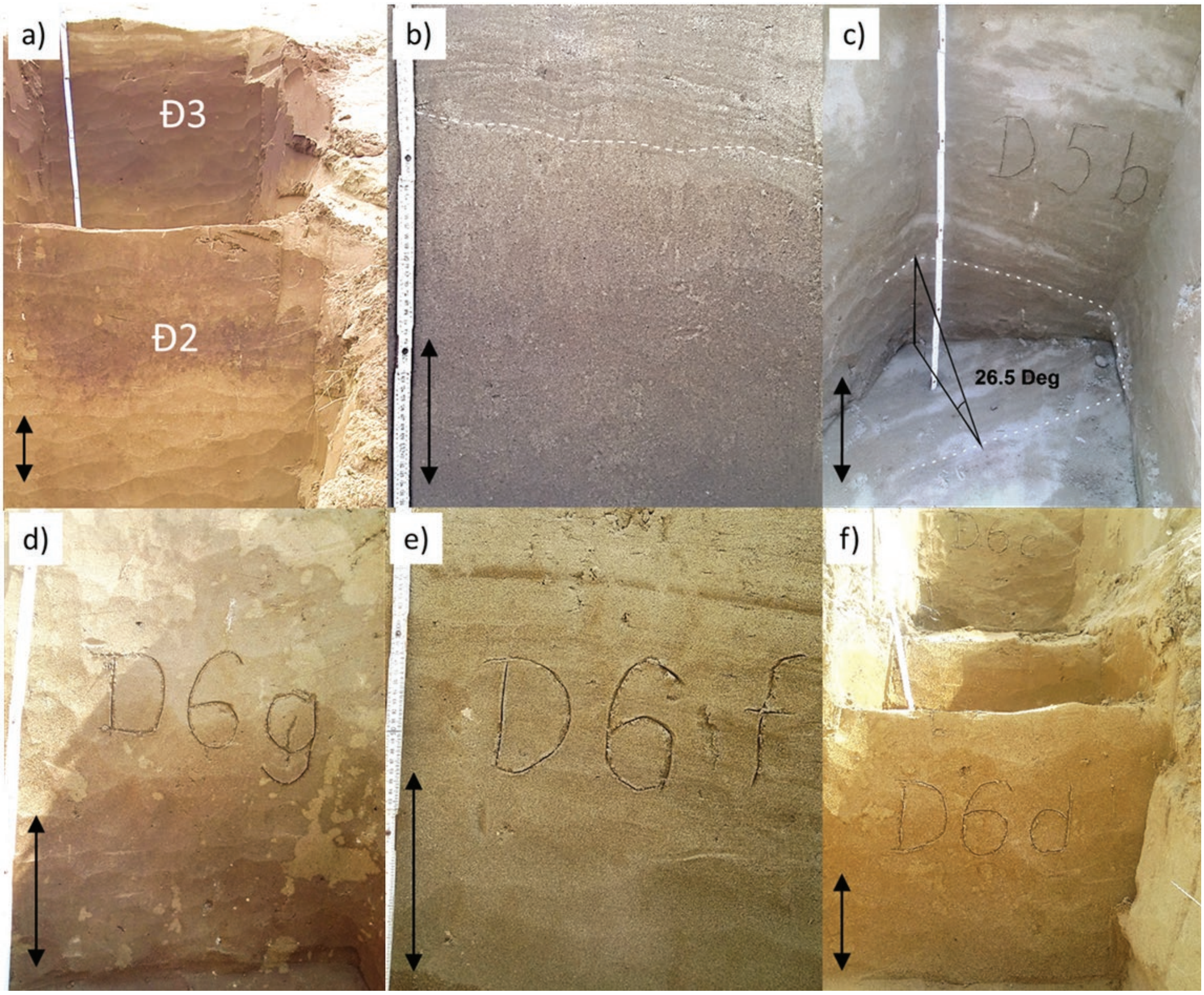

Fig. 4. Photographs of various investigated paleosoil horizons and sand layers portrayed on Fig. 3. **a** — Observation point X; it can clearly be seen that the paleosoil actually consists of two individual soils. **b** — Observation point D1; the dashed line shows the boundary between the bioturbated unstratified paleosoil (below) and laminated dune sands (above). **c** — Observation point D5b, showing oblique parallel laminated dune sand with a dipping angle of 26.5°, several meters below the pedocomplex. **d** — Observation point D6g, showing the bioturbated and unstratified paleosoil horizon just below D6f. **e** — Observation point D6f, showing oblique parallel laminated dune sands. **f** — Observation point D6d, showing a potential younger paleosoil buried underneath D6c (see text). The length of the two-sided arrow is 20 cm.

Table 1: Sample ID, depth and colour (the latter according to the Munsell Soil Color Book 2013). The horizontal profile samples, which represent the pedocomplex, are marked by an asterisk (*).

Sample	Sampling depth (m a.s.l.)	Munsell Colour (2013)	
D1*	119.0	10 YR 4/3	Brown
D2*	119.0	10 YR 3/4	Dark yellowish brown
D3*	119.5	7.5 YR 3/2	Dark brown
D4*	119.7	10 YR 3/2	Very dark greyish brown
D5a*	119.5	10 YR 3/3	Dark brown
D5b	116.1	2.5 Y 5/3	Light olive brown
D6a	123.5	2.5 Y 4/4	Olive brown
D6b	123.0	10 YR 4/4	Dark yellowish brown
D6c	122.3	10 YR 4/4	Dark yellowish brown
D6d	121.5	10 YR 4/4	Dark yellowish brown
D6e	120.8	10 YR 4/3	Brown
D6f	120.1	2.5 Y 4/3	Olive brown
D6g*	119.4	7.5 YR 4/3	Brown
D6h*	118.9	7.5 YR 3/2	Dark brown
D6i	118.2	2.5 Y 5/3 10 YR 5/3	Light olive brown Brown
D7*	120.0	10 YR 3/4	Dark yellowish brown
D8*	119.7	10 YR 4/3 10 YR 3/3	Brown - Dark brown
P-soil horizons		7.5-10YR 3-4/2-4	
Sand layers		2.5Y-10YR 4-5/3-4	

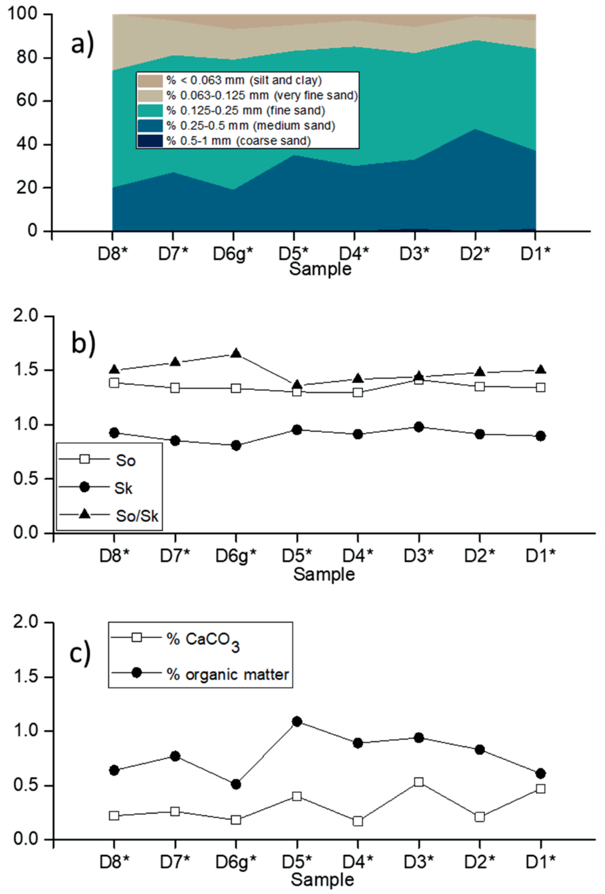

Radiocarbon dating

In summary, the ages were calculated as 13.566±229 cal yr BP and 14.659±498 cal yr BP for the lower and upper paleosoil, respectively (Table 2, Fig. 7), which corresponds with the Bølling–Allerød interstadial period (BA), roughly situated between 14.7 and 12.9 ka BP (Late Pleistocene; Fig. 7).

Discussion

Origin of cross-strata

According to Hećimović (1987), during the Holocene, the Drava River fluvial sediments (N Croatia) were repeatedly reworked by wind and resedimented in the form of dunes (the Đurđevac Sands). However, unexpectedly, the radiocarbon dating analysis showed that the two intraformational paleosoils developed before the Holocene. According to the Weichselian chronostratigraphy (Protin et al. 2021), the older paleosoil developed at the beginning, and the younger paleosoil in the middle part of the Bølling–Allerød interstadial period (BA; Fig. 7).

The sediments above and below the paleosoils clearly show oblique parallel lamination. The inclination of the sand in horizon D5b is 26.5°, suggesting that the Late Pleistocene sediment directly underlying the paleosoils is aeolian dune sand (Fig. 4c).

Pye and Tsoar (2009) suggest distinguishing aeolian sands from beach and fluvial sands based on mean size, sorting, and skewness. According to Ahlbrandt's investigation (1979), which compiled mean size and sorting data for 464 inland and coastal dune samples, the mean size is predominantly in the fine sand range (0.125–0.25 mm), and sands are moderately well sorted. In this research, the deposits consist almost exclusively of sand-sized grains in the fraction between 0.5 and 0.125 mm (medium and fine sand), while silt and clay are almost completely absent. In 11 out of 17 samples, the fine sand fraction dominates. The median grain size is always between 0.18 mm and 0.25 mm, with an average of 0.21 ±0.02 mm for soil horizons and 0.24±0.03 mm for sand layers (Appendix 1), while a range of 0.15–0.25 mm is typical for aeolian dune deposits (Tišljar 2004). The sorting coefficient ranges between 1.20 and 1.41, with an average of 1.35 ±0.04 for soil horizons and 1.28±0.07 for sand layers (Appendix 1), while values of less than 1.25 are typical for aeolian dune sands (Tišljar 2004), a value that is consistent with most of the sand layers.

It is not clear yet if Drava River fluvial sediment is present below the aeolian dune sand as it was assumed by Hećimović (1987). If we accept the early BA radiocarbon age of the lower

◄

Fig. 5. Results of analyses on the horizontal profile. **a** — Grain size (%). **b** — Sorting (So) and skewness (Sk). **c** — $CaCO_3$ and organic matter (%). Paleosoil samples are indicated by an asterisk (*).

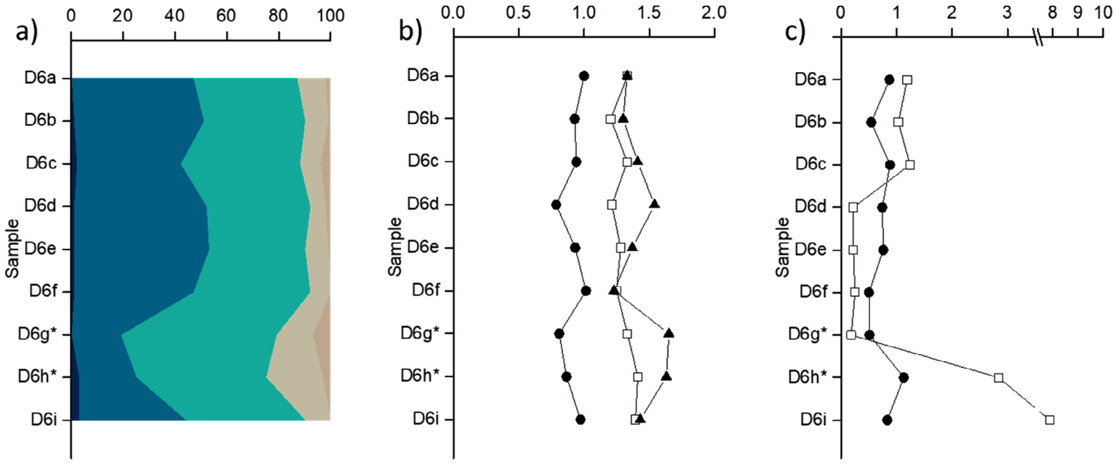

Fig. 6. Results of analyses on the vertical trench. **a** — Grain size (%). **b** — Sorting (So) and skewness (Sk). **c** — $CaCO_3$ and organic matter (%). Paleosoil samples are indicated by an asterisk (*). See Fig. 5 for legend.

Table 2: Radiocarbon dating results. The calibrated radiocarbon age is quoted with a 2σ error margin.

Sample	Sampling depth (m a.s.l.)	Sample type	Fraction of modern radiocarbon		Radiocarbon age		Radiocarbon age cal yr BP
			pMC	1σ error	BP	1σ error	
Đ3	119.7	charcoal	21.14	0.14	12483	53	13.566±229
Đ2	119.1	charcoal	23.29	0.16	11705	55	14.659±498

paleosoil, the aeolian dune sands beneath it date back to the Pleniglacial. During that dry and cold period, the Drava River was continuously providing sufficient sandy material (Hećimović 1987) and aeolian resedimentation could form the dunes.

Fluvial geometries such as gullies or stream channels are lacking, as well as ripples and fining-upward sequences typical for meandering point bars and braided channel bars (Miall 1996; Tišljar 2004; Tucker 2008). The poor roundness of the sand grains suggests short transport distances, most likely the redeposition of Drava River fluvial sediments. Modern Drava River sediment in the vicinity of Đurđevac is dominated by coarse and medium gravel (mean d_{60} diameter is 6.74, min.: 2.2 mm, max.: 11.6 mm). The grain size distributions for ten gravel pits in the Drava River valley between Ormož (Slovenian–Croatian border) and Đurđevac include a gravel pit close to the investigated area (Gazarek et al. 1990). Fluvial sediment comprises equal portions of sand and gravel ranging from 0.1 to 31.5 mm. That significantly differs from sand dunes investigated in this research, however, it could be the source of the material.

The higher sphericity of grains in the southern profile samples (D1–D5a) and the upper part of the trench (D6a–D6e), as well as the low sphericity of grains of older and northern samples could be an indicator of two different sets of laminae, possibly representing two different dune phases. Such a difference between those sample groupings can also be seen in the grain size, the So/Sk ratio, and the organic matter content (Appendix 1, 2, and 3, Figs. 5 and 6). There is a general trend of finer grain size northward, with a switch in sample D5a (Fig. 6a). Possible sedimentological and geomorphological factors that influence lateral grain-size variations will be investigated in the future. Furthermore, when comparing coastal and river valley dunes, coastal inland dunes have more rounded, spherical grains than river valley dunes, since the former are mainly younger and have not been transported a great distance from their source (Pye & Tsoar 2009).

The So/Sk switch in the horizontal profile (Fig. 6b) coincides with the grain size and sphericity trends. The So/Sk ratio has previously been applied as an indicator of the degree of pedological development of paleosoils (Galović 2014). In paleosoil horizons that developed in loess, So/Sk ratios exceed 2.2, while here, the dated paleosoils (D6g and D6h) have a So/Sk ratio of 1.6–1.7 (Fig. 6b). Because of different parent material (loess and dune sand), these ratios cannot be compared, nor can conclusions regarding intensity and duration of soil formation be made. However, the presence of a younger paleosoil (D6d; Fig. 6b) might be presumed, given the rather high So/Sk score for that horizon. In order to distinguish fluvial (Pirkhoffer et al. 2021; Zakwan et al. 2022) and aeolian dunes, Pye and Tsoar (2009) propose multiple discriminant analyses. Peh et al. (1998, 2008) conducted discriminant analysis as a tool for the distinction of Quaternary sediments in the region of Đurđevac and multiple discriminant analyses of the Drava River alluvial plain sediments. Utilizing the geochemical and modal composition as the predictor variables, the authors concluded that Holocene aeolian sediments and Holocene facies of the Drava River (Fig. 2)

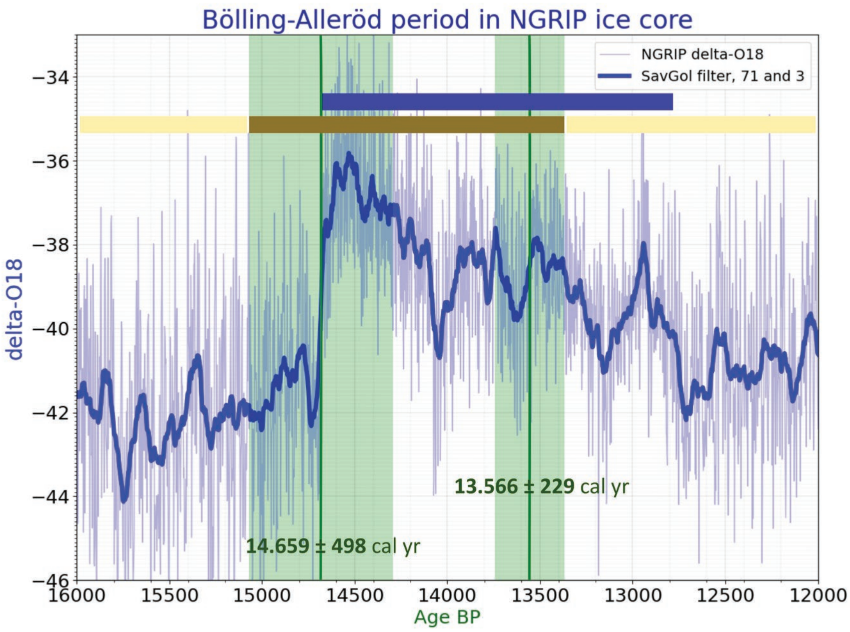

Fig. 7. Radiocarbon ages of the investigated paleosoils (charcoal) put in the geochronological framework of the North Greenland Ice Core Project Oxygen Isotope Data (http://www.iceandclimate.nbi.ku.dk/data/NGRIP_d18O_and_dust_5cm.xls). Blue bar represents the time window of the entire Bølling–Allerød interstadial, brown bar indicates the time period of soil formation (including 2σ errors), and yellow bar shows the potential age windows for sand movement given the range of the x-axis.

remarkably overlap, which proves the same origin of the material. The thickness of aeolian oblique sets is generally greater (usually several meters) compared to underwater dunes (a few dm to 1 m; Allen 1968; Leclair & Bridge 2001; Tišljar 2004; Ashworth et al. 2011).

The origin of the pedocomplex

Overall, the pedocomplex, which we tentatively denote as Kalinovac pedocomplex, presents itself as a set of two weakly-developed paleosoils. They are often merged, with a slightly finer grain size compared to the parent material and a slightly less intensive (chroma) and darker (value) colour. In particular, the upper horizons of the paleosoil complex contain significantly less carbonates than the deeper horizons, which might be due to intraformational decalcification (Van Breemen & Protz 1988; Van Den Berg & Loch 2008). The organic matter content is, statistically speaking, no different from the overlying and underlying sand layers. Hence, the darker colour of the paleosoil horizons is probably a grain size effect and/or due to secondary precipitates, such as ferrous and/or manganese oxides or hydroxides, rather than the result of an increased organic carbon content.

The paleosoils have no clear diagnostic horizons and qualify as (paleo-)arenosols, which is also the dominant recent soil type in the area. Recent forest arenosols in the area have an organic horizon (Oh) 1–3 cm thick and a humus horizon (Ah) up to 10 cm. At control sites, without forest vegetation, arenosols are very low in humus and very thin (up to 2 cm; Vrbek et al. 2017). In general, arenosols are typical soils that developed on recent dunes in arid to humid and per humid climates, ranging from extremely cold to extremely hot. Accordingly, the vegetation ranges from a desert over scattered vegetation (mostly grassy) to light forest. They exhibit only a partially-formed surface horizon (uppermost layer) low in humus content, and they are bereft of subsurface clay accumulation. Today, arenosols occupy about 7 percent of the continental surface area of the Earth (IUSS Working Group WRB 2015).

Paleoclimatic implications

Late Pleistocene and earliest Holocene sand movements are land forming processes that were widespread in many inland regions in Europe. Fluvial processes often play a key role in pre-sorting and concentrating the products of weathering before aeolian processes take place (Smith 1982; Bullard & Livingstone 2002; Pye & Tsoar 2009). For instance, phases of alternating landscape instability and stability have been documented in the Deliblato Sands in Serbia (Menković 2013; Sipos et al. 2016, 2022), eolian deposits in Slovakia (Šujan et al. 2022), and various sand regions in Hungary (Gábris et al. 2012; Buró et al. 2016). In this research, the LGM was important for sand movements as a cold and dry period, and the following BA led to an increase in humidity, which likely relates to the paleoenvironmental changes observed in the depositional record (Fig. 7). The dunes of the Deliblato Sands are supplied from the fluvial sediments of the Danube River (Pannonian basin). On the other side of the world, the spatial distribution and formation mechanism of aeolian dunes in the Yarlung Zangbo Valley led to the conclusion that the wide valleys of the Yarlung River (Tibet) not only provide spaces to accommodate the aeolian deposits, but more importantly, supply fluvial sands to feed the aeolian dunes (Bullard & Livingstone 2002; Liu et al. 2019; Wang et al. 2021). Each mentioned river system valley is characterised by a highly sinuous meandering river (Menković 2013; Sipos et al. 2016, 2022; Liu et al. 2019; Wang et al. 2021).

Phases of landscape stability are deduced from the absence of aeolian activity and the presence of paleosoils. Radiocarbon dates from intraformational paleosoils suggest that soil formations were a common phenomenon during the BA oscillation in large parts of the Carpathian Basin (Buró et al. 2016). Later, during the Holocene, such alternation between sand movement and soil formation continued, but to a lesser extent. This is also the case for the Đurđevac Sands. From historical sources, it is known that these sands were a real threat to agricultural practices and settlements in the Podravina area due to their instability. During dry years, the sand was unsuitable for rooting. Settling of the sands was achieved, mainly by afforestation, only at the end of the 19th and early 20th centuries (Petrić 2009; Bilandžija et al. 2017).

Conclusion

This work aimed to establish the scientific background for determining the age of the Đurđevac Sands and to reveal paleoclimatic dynamics during the last abrupt climate transition from the Pleistocene to Holocene. Radiocarbon ages of charcoal from buried paleosoils indicate that the Đurđevac Sands had formed, at least partially, during the Late Pleistocene, in contradiction to previously published views. The sands appearing below and above the paleosoils clearly show oblique parallel lamination with an angle typical for dune forests. They predominantly consist of fine- to medium-grained sand grains and are well- to very well-sorted. The calcium carbonate content varies, but seems to be (much) higher in the deeper parts of the dune sands. The intraformational pedocomplex actually consists of two individual soil horizons, which may represent two individual soils that merge into one at various locations. The pedocomplex was formed during the Bølling–Allerød warming, an abrupt interstadial period that occurred during the final stages of the last glacial period, roughly between 14.7 and 12.9 ka BP. The pedogenetic evolution of the paleosoil(s), which is tentatively interpreted as an arenosol, is very weak, and it only stands out because of its slightly darker and less intensive colour compared to the underlying and overlying dune sands. It contains slightly more fine sand and several percentages of silt and clay, a fraction that is usually completely lacking in the dune sands themselves. The granulometric coefficient So/Sk (sorting divided by skewness) seems to be a good indicator to identify paleosoils in these sands – it suggests that more intraformational paleosoils than hitherto observed may be present. Furthermore, this work identified a previously unrecognized regional climatic period which interrupted the aeolian deposition. In the future, a detailed, optically-stimulated luminescence sampling campaign is foreseen to elaborate the geochronological framework for the Đurđevac Sands.

Acknowledgments: This work has been fully supported by the Croatian Science Foundation under the projects SAPIQ [4425], ACCENT [3274] and DOK-2021-02-9476. We are grateful to the reviewers for their thorough reviews, which greatly improved the manuscript.

References

Ahlbrandt T.S. 1979: Textual Parameters of Eolian Deposits. In: McKee E.D. (Ed.): A Study of Global Sand Seas. *U.S. Geological Survey* 1052, 21–51.

Allen J.R.L. 1968: Current ripples. *North Holland Publishing Co.*, Amsterdam, 1–433.

Ashworth P.J., Smith G.H.S., Best J.L., Bridge J.S., Lane S.N., Lunt I.A., Reesink A.J.H., Simpson C.J. & Thomas R.E. 2011: Evolution and sedimentology of a channel fill in the sandy braided South Saskatchewan River and its comparison to the deposits of an adjacent compound bar. *Sedimentology* 58, 1860–1883. https://doi.org/10.1111/j.1365-3091.2011.01242.x

Banak A., Pikelj K., Lužar-Oberiter B. & Kordić B. 2021: The sedimentary record of Pleistocene aeolian – alluvial deposits on Vrgada Island (eastern Adriatic coast, Croatia). *Geologia Croatica* 74, 127–137. https://doi.org/10.4154/gc.2021.14

Bašić F. & Feletar D. (Eds.) 2017: Zbornik sažetaka sa Znanstvenog skupa Đurđevački pijesci – geneza, stanje i perspektive [Proceedings of the Scientific Symposium Đurđevac Sands – genesis, state and future]. *Croatian Academy of Sciences and Arts, Institute for Scientific Research and Artistic Work in Križevci*, Zagreb-Križevci, 1–24 (in Croatian).

Bilandžija D., Bašić F., Kisić I., Mesić M., Zgorelec Ž., Šestak I., Perčin A. & Bogunović I. 2017: Agroklimatski pokazatelji kao indikator klimatskih promjena na Đurđevačkim pijescima [Agro climatic characteristics as indicators of climate change in the area of Đurđevac Sands]. In: Bašić F. & Feletar D. (Eds.): Zbornik sažetaka sa Znanstvenog skupa Đurđevački pijesci – geneza, stanje i perspektive [Proceedings of the Scientific Symposium Đurđevac Sands – genesis, state and future]. *Croatian Academy of Sciences and Arts, Institute for Scientific Research and Artistic Work in Križevci*, Zagreb-Križevci, 9 (in Croatian).

Bognar A. 2008: Geomorfološka obilježja korita rijeke Drave i njenog poloja u širem području naselja Križnica [Geomorphologic Characteristics of the Drava River Bed and its Floodplain in Wider Area of the Settlement Križnica]. *Hrvatski geografski glasnik* 70, 49–71 (in Croatian with English abstract). https://doi.org/10.21861/hgg.2008.70.02.03

Bronk Ramsey C. 2009: Bayesian analysis of radiocarbon dates. *Radiocarbon* 51, 337–360. https://doi.org/10.1017/S0033822200033865

Bullard J.E. & Livingstone I. 2002: Interactions between Aeolian and Fluvial Systems in Dryland Environments. *Area* 34, 8–16. http://www.jstor.org/stable/20004201

Buró B., Sipos G., Loki J., Andrasi B., Felegyhazi E. & Negyesi G. 2016: Assessing Late Pleistocene and Holocene phases of aeolian activity on the Nyírség alluvial fan, Hungary. *Quaternary International* 425, 183–195. https://doi.org/10.1016/j.quaint.2016.01.007

Europe Relief Map: maps-for-free.com (Accessed June 21, 2022)
Franjo I. 1997: Geomorfološke osobine Molvarskih Pijesaka. *Podravski Zbornik* 23, 205–218 (in Croatian with English abstract).
Gábris G., Horváth E., Novothny Á. & Ruszkiczay-Rüdiger Z. 2012: Fluvial and aeolian landscape evolution in Hungary – results of the last 20 years research. *Netherlands Journal of Geosciences – Geologie en Mijnbouw* 91, 111–128. https://doi.org/10.1017/S0016774600001530
Galović L. 2014: Geochemical archive in the three loess/paleosol sections in the Eastern Croatia: Zmajevac I, Zmajevac and Erdut. *Aeolian Research* 15, 113–132. https://doi.org/10.1016/j.aeolia.2014.07.004
Galović L. 2016: Sedimentological and mineralogical characteristics of the Pleistocene loess/paleosol sections in the Eastern Croatia. *Aeolian Research* 20, 7–23. https://doi.org/10.1016/j.aeolia.2015.10.007
Galović L. & Peh Z. 2014: Eolian contribution to geochemical and mineralogical characteristics of some soil types in Medvednica Mountain, Croatia. *Catena* 117, 145–156. https://doi.org/10.1016/j.catena.2013.12.016
Galović L. & Posilović H. 2017: Geneza i značenje eolskih naslaga Podravine [Genesis and significance of aeolian deposits of the Podravina area]. In: Bašić F. & Feletar D. (Eds.): Zbornik sažetaka sa Znanstvenog skupa Đurđevački pijesci – geneza, stanje i perspektive [Proceedings of the Scientific Symposium Đurđevac Sands – genesis, state and future]. *Croatian Academy of Sciences and Arts, Institute for Scientific Research and Artistic Work in Križevci*, Zagreb-Križevci, 3 (in Croatian).
Galović L., Frechen M., Halamić J., Durn G. & Romić M. 2009: Loess chronostratigraphy in Eastern Croatia – A first luminescence dating approach. *Quaternary International* 198, 85–97. https://doi.org/10.1016/j.quaint.2008.02.004
Galović L., Frechen M., Peh Z., Durn G. & Halamić J. 2011: Loess/palaeosol section in Šarengrad, Croatia – A qualitative discussion on the correlation of the geochemical and magnetic susceptibility data. *Quaternary International* 240, 22–34. https://doi.org/10.1016/j.quaint.2011.02.003
Galović L., Beerten K., Šorša A., Poch R.M., Stejić P., Gajić R., Pandurov M. & Husnjak S. 2021: Incoming research project: Abrupt climate changes – Evidence from Quaternary sedimentological sequences in Croatia (ACCENT). In: Jamšek Rupnik P. & Novak A. (Eds.): Book of abstracts. 6th Regional Scientific Meeting on Quaternary Geology: Seas, Lakes and Rivers. *Geological Survey of Slovenia*, Ljubljana, 24–25.
Galović L., Beerten K. & Posilović H., in press a: The age of the Đurđevac Sands (Podravina, N Croatia). In: Ksibi M., Negm A., Hentati O., Ghorbal A., Sousa A., Rodrigo-Comino J., Panda S., Lopes Velho J., El-Kenawy A.M., Perilli N., Michaud P., Hadji R., Guerriero G., Arfi R.B., Suaria G., Candamano S., Khadhraoui M., Jebari S. & Falcinelli S. (Eds.): Proceedings of the 3rd Euro-Mediterranean Conference for Environmental Integration, Tunisia. *Springer*, Berlin.
Galović L., Beerten K., Šorša A., Poch R.M., Stejić P., Gajić R., Pandurov M. & Husnjak S., in press b: Incoming research project: Abrupt climate changes – Evidence from Quaternary sedimentological sequences in Croatia (ACCENT). In: Ksibi M., Negm A., Hentati O., Ghorbal A., Sousa A., Rodrigo-Comino J., Panda S., Lopes Velho J., El-Kenawy A.M., Perilli N., Michaud P., Hadji R., Guerriero G., Arfi R.B., Suaria G., Candamano S., Khadhraoui M., Jebari S. & Falcinelli S. (Eds.): Proceedings of the 3rd Euro-Mediterranean Conference for Environmental Integration, Tunisia. *Springer*, Berlin.
Gazarek M., Crnički J., Premur V. & Kreč D. 1990: Grain size of gravels, sands and heavy minerals in the sands of the Drava River basin between Ormož and Đurđevac. *Rudarsko-geološki-naftni zbornik* 2, 67–73 (in Croatian with English abstract).
Hećej N. & Durn G. 2021: Properties of the Upper Part of the Last Glacial Loess-Palaeosol Sequence at Savudrija (Istria, Croatia). In: Jamšek Rupnik P. & Novak A. (Eds.): Book of abstracts. 6th Regional Scientific Meeting on Quaternary Geology: Seas, Lakes and Rivers. *Geological Survey of Slovenia*, Ljubljana, 33–34.
Hećimović I. 1987: Osnovna geološka karta SFRJ 1:100.000. Tumač za list Đurđevac L33–71 [Basic geological map of SFRY, scale 1:100.000, Guidebook of the geological map for the Đurđevac sheet]. *Federal Geological Survey*, Belgrade, 1–39 (in Croatian).
Hećimović I. 1988: Osnovna geološka karta SFRJ 1:100.000, list Đurđevac L33–71 [Basic geological map of SFRY, scale 1:100.000, Sheet Đurđevac L33–71]. *Federal Geological Survey,* Belgrade (in Croatian).
HRN ISO 11277:2011 2011: Soil quality – Determination of particle size distribution in mineral soil material – Method by sieving and sedimentation (ISO 11277:2009).
IUSS Working Group WRB 2015: World Reference Base for Soil Resources 2014, update 2015 International soil classification system for naming soils and creating legends for soil maps. World Soil Resources Reports No. 106. *FAO*, Rome, 1–192.
Krumbein W. & Sloss L. 1963: Stratigraphy and Sedimentation. *W.H. Freeman and Co*., San Francisco, 1–660.
Leclair S.F. & Bridge J.S. 2001: Quantitative interpretation of sedimentary structures formed by river dunes. *Journal of Sedimentary Research* 71, 713–716. https://doi.org/10.1306/2DC40962-0E47-11D7-8643000102C1865D
Liu Y., Wang Ys. & Shen T. 2019: Spatial distribution and formation mechanism of aeolian sand in the middle reaches of the Yarlung Zangbo River. *Journal of Mountain Science* 16, 1987–2000. https://doi.org/10.1007/s11629-019-5509-5
Menković L. 2013: Eolian relief of southeast Banatian. *Bulletin of the Serbian geographical society* 93, 1–22. https://doi.org/10.2298/GSGD1304001M
Miall A.D. 1996: The Geology of Fluvial Deposits: Sedimentary Facies, Basin and Petroleum Geology. *Springer-Verlag*, Berlin-Heidelberg, 1–616.
Munsell Soil Color Book 2013: Munsell Soil Color Charts with genuine Munsell color chips. *Macbeth Division of Kollmorgem Instruments Corporation*, New Windsor.
Müller G. 1967: Methods in Sedimentary Petrology. Sedimentary Petrology, Part I. *Schweizerbart*, Stuttgart, 1–283.
North Greenland Ice Core Project Members 2004: High-resolution record of Northern Hemisphere climate extending into the last interglacial period (http://www.iceandclimate.nbi.ku.dk/data/NGRIP_d18O_and_dust_5cm.xls). *Nature* 431, 147–151, https://doi.org/10.1038/nature02805 (Accessed February 28, 2022).
Pavelić D. 2001: Tectonostratigraphic model for the North Bosnian Sector of the Miocene Pannonian Basin System. *Basin Research* 12, 359–376. https://doi.org/10.1046/j.0950-091x.2001.00155.x
Peh Z., Novosel-Škorić S. & Kruk Lj. 1998: Discriminant Analysis as a Tool for the Distinction of Quaternary Sediments in the Region of Đurđevac. *Geologia Croatica* 51, 47–58. https://doi.org/10.4154/GC.1998.07
Peh Z., Šajn R., Halamić J. & Galović L. 2008: Multiple discriminant analysis of the Drava River alluvial plain sediments. *Environmental Geology* 55, 1519–1535. https://doi.org/10.1007/s00254-007-1102-2
Petrić H. 2009: Fluvial-aeolian sands in Croatia. *Podravina* 8, 89–97. https://hrcak.srce.hr/77750 (Accessed May 20, 2022)
Pirkhoffer E., Halmai Á., Ficsor J., Gradwohl-Valkay A., Lóczy D., Nagy Á., Liptay Z.Á. & Czigány S. 2021: Bedload entrainment dynamics in a partially channelized river with mixed bedload: A case study of the Drava River, Hungary. *River Research and Applications* 37, 699–711. https://doi.org/10.1002/rra.3794

Pola M., Pavičić I., Rubinić V., Kosović I., Galović L., Borović S., Wacha L. & Urumović K. 2020: First results of multidisciplinary investigations for the hydrogeological conceptual modelling of loess deposits in eastern Croatia. *Acque Sotterranee – Italian Journal of Groundwater* 9, 43–49. https://doi.org/10.7343/as-2020-432

Prelogović E., Saftić B., Kuk V., Velić J., Dragaš M. & Lučić D. 1998: Tectonic activity in the Croatian part of the Pannonian basin. *Tectonophysics* 297, 283–293. https://doi.org/10.1016/S0040-1951(98)00173-5

Protin M., Schimmelpfennig I., Mugnier J.-L., Buoncristiani J.-F., Le Roy M., Pohl B., Moreau L. & ASTERTeam 2021: Millennial-scale deglaciation across the European Alps at the transition between the Younger Dryas and the Early Holocene – evidence from a new cosmogenic nuclide chronology. *Boreas* 50, 671–685. https://doi.org/10.1111/bor.12519

Pye K. & Tsoar H. 2009: Aeolian sand and sand dunes. *Springer*, Berlin, 1–458. https://doi.org/10.1007/978-3-540-85910-9

Reimer P.J., Austin W.E.N., Bard E., Bayliss A., Blackwell P.G., Bronk Ramsey C., Butzin M., Cheng H., Edwards R.L., Friedrich M., Grootes P.M., Guilderson T.P., Hajdas I., Heaton T.J., Hogg A.G., Hughen K.A., Kromer B., Manning S.W, Muscheler R., Palmer J.G., Pearson C., van der Plicht J., Reimer R.W., Richards D.A., Scott E.M., Southon J.R., Turney C.S.M., Wacker L., Adolphi F., Büntgen U., Capano M., Fahrni S.M., Fogtmann-Schulz A., Friedrich R., Köhler P., Kudsk S., Miyake F., Olsen J., Reinig F., Sakamoto M., Sookdeo A. & Talamo S. 2020: The IntCal20 Northern Hemisphere radiocarbon age calibration curve (0–55 cal kBP). *Radiocarbon* 62, 725–757. https://doi.org/10.1017/RDC.2020.41

Romić M., Bragato G., Zovko M., Romić D., Mosetti D., Galović L. & Bakić H. 2014: The characteristics of cultivated soils developed from coastal paleosand (Korčula Island, Croatia). *Catena* 113, 281–291. https://doi.org/10.1016/j.catena.2013.08.009

Rubinić V., Galović L., Husnjak S. & Durn G. 2015: Climate vs. parent material – Which is the key of Stagnosol diversity in Croatia? *Geoderma* 241, 250–261. https://doi.org/10.1016/j.geoderma.2014.11.029

Rubinić V., Galović L., Lazarević B., Husnjak S. & Durn G. 2018: Pseudogleyed loess derivates – The most common soil parent materials in the Pannonian region of Croatia. *Quaternary International* 494, 248–262. https://doi.org/10.1016/j.quaint.2017.06.044

Sipos G., Marković,S., Tóth O., Gavrilov M., Balla A., Kiss T., Urdea P. & Mészáros M. 2016: Assessing the morphological characteristics and formation time of the Deliblato Sands, Serbia. *Geophysical Research Abstracts* 18, EGU2016-13752.

Sipos G., Marković S., Gavrilov M., Balla A., Filyó D., Bartyik T., Mészáros M., Tóth O., van Leeuwen B., Lukić T., Urdeac P. Onacac A. & Kiss T. 2022: Late Pleistocene and Holocene aeolian activity in the Deliblato Sands, Serbia. *Quaternary Research* 107, 113–124. https://doi.org/10.1017/qua.2021.67

Smith R.S.U. 1982: Sand dunes in the North American desert. In: Bender G.L. (Ed.): Reference handbook on the deserts of North America. *Greenwood Press*, Westport, 481–526.

Šujan M., Rybár S., Thamó-Bozsó E., Klučiar T., Tibenský M. & Sebe K. 2022: Collapse wedges in periglacial eolian sands evidence Late Pleistocene paleoseismic activity of the Vienna Basin Transfer Fault (western Slovakia). *Sedimentary Geology* 431, 106103. https://doi.org/10.1016/j.sedgeo.2022.106103

Taylor R.E. 1987: Radiocarbon Dating: An Archaeological Perspective. *Academic Press*, New York, 1–224. https://doi.org/10.1016/B978-0-126-84860-1.X5001-6

Tišljar J. 2004: Sedimentologija klastičnih i silicijskih taložina [Sedimentology of clastic and silicate sediments]. *Institut za geološka istraživanja*, Zagreb, 1–426 (in Croatian).

Tucker M.E. 2008: Sedimentary Petrology – An Introduction to the Origin of Sedimentary Rocks. 3rd Edition. *Wiley Blackwell*, 1–261.

Van Breemen N. & Protz R. 1988: Rates of calcium carbonate removal from soils. *Canadian Journal of Soil Science* 68, 449– 454.

Van Den Berg G.A. & Loch J.P.G. 2008: Decalcification of soils subject to periodic waterlogging. *European Journal of Soil Science* 51, 27–33. https://doi.org/10.1046/j.1365-2389.2000.00279.x

Vandenberghe D.A.G., Derese C., Kasse C. & Van Den Haute P. 2013: Late Weichselian (fluvio-)aeolian sediments and Holocene drift-sands of the classic type locality in Twente (E Netherlands): a high-resolution dating study using optically stimulated luminescence. *Quaternary Science Reviews* 68, 96–113. https://doi.org/10.1016/j.quascirev.2013.02.009

Vrbek B., Pernar N., Bakšić D. & Perković I. 2017: Neke pedološke značajke ekosustava Đurđevačkih pijesaka [Some pedological features of the Đurđevac Sands ecosystem]. In: Bašić F. & Feletar D. (Eds.): Zbornik sažetaka sa Znanstvenog skupa Đurđevački pijesci – geneza, stanje i perspektive [Proceedings of the Scientific Symposium Đurđevac Sands – genesis, state and future]. *Croatian Academy of Sciences and Arts, Institute for Scientific Research and Artistic Work in Križevci*, Zagreb-Križevci, 8 (in Croatian).

Wacha L., Galović L., Koloszár L., Magyari Á., Chikán G. & Marsi I. 2013. The chronology of the Šarengrad II loess-palaeosol section (Eastern Croatia). *Geologia Croatica* 66, 191–203. https://doi.org/10.4154/GC.2013.18

Wacha L., Matoš B., Kunz A., Lužar-Oberiter B., Tomljenović B. & Banak A. 2018: First post-IR IRSL dating results of Quaternary deposits from Bilogora (NE Croatia): Implications for the Pleistocene relative uplift and incision rates in the area. *Quaternary International* 494, 193–210. https://doi.org/10.1016/j.quaint.2017.08.049

Wang B., Gong J., Zuza A.V., Liu R., Bian S., Tian Y., Yang X., Zhang D. & Chen H. 2021: Aeolian sand dunes alongside the Yarlung River in southern Tibet: A provenance perspective. *Geological Journal* 56, 2625–2636. https://doi.org/10.1002/gj.4058

Wentworth C.K. 1922: A scale of grade and class terms for clastic sediment. *Journal of Geology* 30, 377–392. https://doi.org/10.1086/622910

Zakwan M., Pham Q.B., Bonacci O. & Đurin B. 2022: Application of revised innovative trend analysis in lower Drava River. *Arabian Journal of Geosciences* 15, 758. https://doi.org/10.1007/s12517-022-09591-5

Appendix 1: Grain size composition, coefficients and sorting of grains (Wentworth 1922; Müller 1967). Md = median in mm, So = sorting (dimensionless), Sk = skewness (dimensionless). Grain size given in mm. Samples from the pedocomplex are indicated by an asterisk (*).

Sample	**Grain size coefficients**				**Grain size composition (%)**					**Sediment type**	**Sorting**
	Md	So	Sk	So/Sk	Coarse sand	Medium sand	Fine sand	Very fine sand	Silt and clay		
					1–0.5	0.5–0.25	0.25–0.125	0.125–0.063	<0.063		
D1*	0.22	1.34	0.90	1.50	1	36	47	13	3	Fine sand	Good
D2*	0.24	1.35	0.91	1.48	0	47	41	11	1	Medium sand	Good
D3*	0.20	1.41	0.98	1.44	1	32	49	12	6	Fine sand	Moderate
D4*	0.21	1.30	0.91	1.42	0	30	55	12	3	Fine sand	Good
D5a*	0.22	1.30	0.95	1.36	0	35	48	12	3	Fine sand	Good
D5b	0.18	1.22	0.96	1.28	0	12	70	16	2	Fine sand	Very good
D6a	0.24	1.33	1.00	1.33	0	47	40	11	2	Medium sand	Good
D6b	0.25	1.20	0.93	1.30	1	50	39	9	1	Medium sand	Very good
D6c	0.24	1.33	0.94	1.41	2	40	46	8	4	Fine sand	Good
D6d	0.26	1.21	0.79	1.54	1	51	40	6	2	Medium sand	Very good
D6e	0.26	1.28	0.93	1.37	1	52	37	9	1	Medium sand	Good
D6f	0.24	1.25	1.02	1.23	1	46	45	8	0	Medium sand	Good
D6g*	0.20	1.33	0.81	1.65	0	19	60	14	7	Fine sand	Good
D6h*	0.19	1.41	0.87	1.63	3	22	50	22	3	Fine sand	Moderate
D6i	0.24	1.39	0.97	1.43	3	41	46	10	0	Fine sand	Good
D7*	0.21	1.34	0.85	1.57	0	27	54	16	3	Fine sand	Good
D8*	0.18	1.39	0.93	1.50	0	20	54	26	0	Fine sand	Good
P-soil horizons	*0.21 ±0.02*	*1.35 ±0.04*	*0.90 ±0.05*	*1.51 ±0.10*	*1±1*	*30±9*	*51±6*	*15±5*	*3.3±2.2*		
Sand layers	0.24 ±0.03	1.28 ±0.07	0.94 ±0.07	1.36 ±0.10	1±1	42±13	45±11	10±3	1.5±1.3		

Appendix 2: Organic matter and inorganic carbon content.

Sample	**Organic matter (%)**	**$CaCO_3$ (%)**
D1*	0.61	0.47
D2*	0.83	0.21
D3*	0.94	0.53
D4*	0.89	0.17
D5a*	1.09	0.4
D5b	0.53	10.66
D6a	0.87	1.19
D6b	0.54	1.03
D6c	0.88	1.24
D6d	0.74	0.22
D6e	0.76	0.22
D6f	0.5	0.25
D6g*	0.51	0.18
D6h*	1.13	2.84
D6i	0.83	7.89
D7*	0.77	0.26
D8*	0.64	0.22
P-soil horizons	*0.82±0.85*	*0.59±0.60*
Sand layers	*0.71±0.16*	2.84±4.06

Appendix 3: Results of the morphologic analysis of sand grains (Krumbein & Sloss 1963). Paleosoil samples are indicated by an asterisk (*).

Sample	Roundness					Sphericity				
	Fraction (mm)				Description	Fraction (mm)				Description
	1–0.5	0.5–0.25	0.25–0.125	0.125–0.09		1–0.5	0.5–0.25	0.25–0.125	0.125–0.09	
D1*	0.27	0.26	0.19	0.24	angular	0.72	0.64	0.68	0.69	moderate sphericity
D2*	0.25	0.23	0.18	0.20	subangular	0.76	0.68	0.67	0.68	moderate sphericity
D3*	0.25	0.21	0.18	0.18	angular	0.71	0.68	0.67	0.61	moderate sphericity
D4*	0.24	0.19	0.17	0.17	angular	0.73	0.69	0.66	0.63	moderate sphericity
D5a*	0.25	0.21	0.17	0.17	angular	0.72	0.66	0.85	0.64	high sphericity
D5b		0.19	0.20	0.24	angular		0.67	0.66	0.67	moderate sphericity
D6a	0.23	0.18	0.17	0.22	angular	0.68	0.63	0.64	0.72	moderate sphericity
D6b	0.23	0.21	0.18	0.17	subangular	0.68	0.65	0.61	0.56	moderate sphericity
D6c	0.25	0.20	0.18	0.18	angular	0.67	0.64	0.65	0.64	moderate sphericity
D6d	0.21	0.17	0.17	0.16	angular	0.67	0.63	0.61	0.60	moderate sphericity
D6e	0.21	0.19	0.18	0.17	angular	0.64	0.62	0.60	0.55	moderate sphericity
D6f	0.20	0.18	0.17	0.16	angular	0.65	0.53	0.58	0.59	low sphericity
D6g*		0.20	0.18	0.16	angular		0.63	0.59	0.63	low sphericity
D6h*	0.24	0.19	0.17	0.18	angular	0.61	0.58	0.57	0.57	low sphericity
D6i	0.25	0.23	0.19	0.17	angular	0.65	0.54	0.59	0.61	low sphericity
D7*		0.16	0.17	0.17	angular		0.57	0.55	0.53	low sphericity
D8*		0.20	0.19	0.19	angular		0.56	0.56	0.55	low sphericity
P-soil horizons	*0.25 ±0.01*	*0.20 ±0.03*	*0.18±0.01*	*0.18±0.2*		0.71 ±0.05	0.63 ±0.05	0.64±0.09	0.61±0.06	
Sand layers	0.23 ±0.02	0.19 ±0.02	0.18±0.01	0.18±0.03		0.66 ±0.02	0.61 ±0.05	0.62±0.03	0.62±0.06	